IOP Publishing Journal of Micromechanics and Microengineering
J. Micromech. Microeng. **17** (2007) N11–N15 doi:10.1088/0960-1317/17/4/N01

NOTE

Capillary flow control using hydrophobic patterns

Ji Won Suk and Jun-Hyeong Cho

LG Chem, Ltd., Research Park, Daejeon, 305-380, Korea

E-mail: stonejws@lgchem.com

Received 7 September 2006, in final form 17 January 2007
Published 22 February 2007
Online at stacks.iop.org/JMM/17/N11

Abstract
This note presents a simple method to control the speed of the autonomous capillary flow using an array of hydrophobic patterns. The microfluidic system in this note was composed of two planar parallel plates that were separated by spacers. The bottom plate had a hydrophilic microchannel which was surrounded by hydrophobic tracks. The top surface was relatively hydrophobic compared to the bottom plate. These hydrophobic tracks and the hydrophobic patterns in the middle of the microchannels were patterned using PDMS stamps by contact printing. By controlling the ratio of hydrophobic area to the whole channel width and the distance between two plates, it was possible to control the capillary flow speed at specific positions. Using this method, it is expected to achieve a sufficient incubation time for biological reactions in microfluidic devices using the capillary flow.

(Some figures in this article are in colour only in the electronic version)

1. Introduction

Control of liquid within microchannels is at the heart of microfluidic systems for chemical, biological and medical applications [1–4]. In recent years, many techniques have been developed for various operations such as metering, transporting, positioning and mixing liquid. These techniques generally rely on active control by mechanical pumping [5, 6], electro-osmotic force [7], electrowetting [8] and magnetic fields [9]. These active controls provide rapid and precise manipulation of small amount of liquid for microfluidic systems. However, these need additional energy sources or equipment such as a mechanical pump, a power supplier, a function generator and a voltage amplifier. This causes the increase of size, cost and complexity of microfluidic devices and several passive control methods have been researched to overcome these drawbacks.

As a passive control method, capillarity or capillary action has been used for microfluidic systems. Capillarity is a natural phenomenon caused by surface tension effects, where liquid wets the interior of capillaries according to adhesion and cohesion forces. When this capillary action is used for microfluidics, the wetting property of microchannels has a significant effect on the liquid behavior. While water autonomously penetrates into a microchannel that has a hydrophilic surface inside it, it does not flow into hydrophobic surfaces without additional pressure. Taking advantage of this effect, it was possible to control the flow of liquid inside microchannels [10], fabricate a microchannel with no wall [11, 12], and make a stop valve using hydrophobic patches [13–16].

Generally, biological reactions need sufficient incubation time to complete the reactions and achieve the maximum signals [17, 18]. However, in previous control methods using capillary flow [10–16], it was required to introduce additional manipulations to resume the flow which was blocked by hydrophobic surfaces. In this respect, if stopping and resuming the motion of the capillary flow are autonomously controlled by 'programmed' microfluidic design, the microfluidic system could be more similar to an ideal system.

In this note, a simple method was proposed to control the autonomous capillary flow with a passive method. The capillary flow can be retarded with appropriate hydrophobic patterns in hydrophilic channel surfaces. The microfluidic system consists of two planar parallel surfaces, separated by spacers. Liquid is confined with hydrophobic tracks with

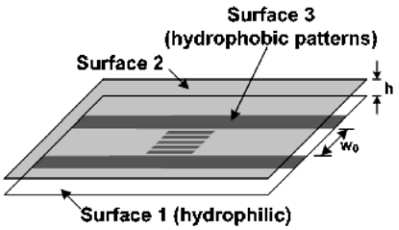

Figure 1. Schematic illustration of a microfluidic system.

no wall and hydrophobic patterns are implemented into a microfluidic channel. Using the array of hydrophobic patterns, it is possible to control the capillary flow speed and get a proper delaying time at specific position in microchannels.

2. Concept

The autonomous liquid filling in microchannels can be explained in terms of energy changes in the solid–liquid–gas interface system [10]. The total interfacial energy of the system, U_T, can be written as follows:

$$U_T = \sum_{i,j,k} \left(A_{S_i L_j} \gamma_{S_i L_j} + A_{S_j G_k} \gamma_{S_j G_k} + A_{L_i G_k} \gamma_{L_i G_k} \right), \qquad (1)$$

where $A_{S_i L_j}$, $A_{S_j G_k}$ and $A_{L_i G_k}$ are solid j-liquid i, solid j-gas k, liquid i-gas k interface areas, respectively, and $\gamma_{S_i L_j}$, $\gamma_{S_j G_k}$ and $\gamma_{L_i G_k}$ are their corresponding surface energies per unit area. The relation between the surface energies and the liquid contact angle $\theta_{C_{ijk}}$ at the solid–liquid–gas interface line is expressed in Young's equation as

$$\gamma_{S_j G_k} = \gamma_{S_j L_i} + \gamma_{L_i G_k} \cos\theta_{C_{ijk}}. \qquad (2)$$

The pressure inside the liquid, P, can be written as a function of the injected liquid volume V_L. Introducing equation (2) into equation (1), the pressure inside the liquid can be expressed as

$$P = -\frac{\mathrm{d}U_T}{\mathrm{d}V_L} = \sum_{i,j,k} \left(\frac{\mathrm{d}A_{L_i G_k}}{\mathrm{d}V_L} - \cos\theta_{C_{ijk}} \frac{\mathrm{d}A_{S_j L_i}}{\mathrm{d}V_L} \right). \qquad (3)$$

The microfluidic system in this note is formed by two planar parallel plates that are separated by a distance h as shown in figure 1. The bottom plate (surface 1) has a hydrophilic microchannel with a width w_0 which is surrounded by hydrophobic tracks (surface 3). These hydrophobic tracks work as a virtual wall to confine a liquid in a microchannel. The top plate (surface 2) is relatively hydrophobic compared to the bottom plate. Hydrophobic patterns position in the middle of the microchannel and each pattern has a rectangular shape with a length L and a width w_1 (figure 2).

When the liquid moves into the microchannel from an inlet hole, three steps can be considered as shown in figure 2. The first step occurs when the liquid flows into the hydrophilic surfaces between two hydrophobic tracks like figure 2(a). The liquid does not spread out due to the relative hydrophobic property of the top surface. In this case, the pressure in the liquid, P_1, can be written using equation (3) as the following.

$$P_1 = \frac{\gamma}{h} \left(\cos\theta_1 + \cos\theta_2 - \frac{2h}{w_0} \right), \qquad (4)$$

where γ is the surface energy of the liquid, θ_1 and θ_2 are the liquid contact angles to the bottom (surface 1) and top (surface 2) surfaces respectively, h is the distance between the top and bottom surfaces, and w_0 is the width of the microchannel. If P_1 has a positive value, the liquid fills the microchannel by capillary force.

The second step is the case when the liquid meets hydrophobic patterns inside the microchannel in figure 2(b). In this case, the average wetting property of the microchannel surface is changed and that influences the pressure in the liquid. We define a parameter, R, which is a ratio of hydrophobic area to the whole channel width:

$$R = \frac{w_1 \times n}{w_0}, \qquad (5)$$

where n is the number of hydrophobic patterns. The pressure in the liquid at the second step, P_2, is written using equations (3) and (5) as the following:

$$P_2 = \frac{\gamma}{h} \left(\cos\theta_1 + \cos\theta_2 + (\cos\theta_3 - \cos\theta_1) R - \frac{2h}{w_0} \right) \qquad (6)$$

where θ_3 is the liquid contact angle to hydrophobic patterns. In equation (6), the value of R ranges from 0 to 1 and $\cos\theta_3$ is negative due to the hydrophobic property of surface 3. Therefore, the pressure at the second step is smaller than that at the first step. When the liquid meets hydrophobic patterns, its speed decreases according to the reduced pressure. In addition, as the distance between two plates, h, increases, P_1 and P_2 decrease according to equations (3) and (6) if the other parameters are fixed.

Finally, when the flow reaches the end of hydrophobic patterns, the pressure in the liquid recovers to that at the first step and this leads the recovery of the flow speed as shown in figure 2(c).

As a result, it is possible to control the speed of the capillary flow in microchannels by implementing an array of hydrophobic patterns.

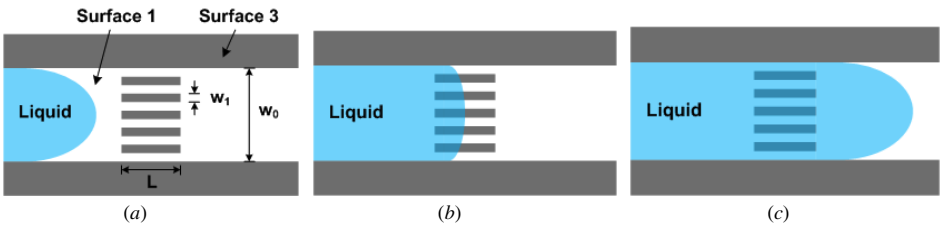

Figure 2. Schematic illustration of autonomous capillary flow in the microfluidic system. (a) Liquid flows along the hydrophilic surface. (b) Liquid meets hydrophobic patterns and is retarded. (c) Liquid passes through hydrophobic patterns.

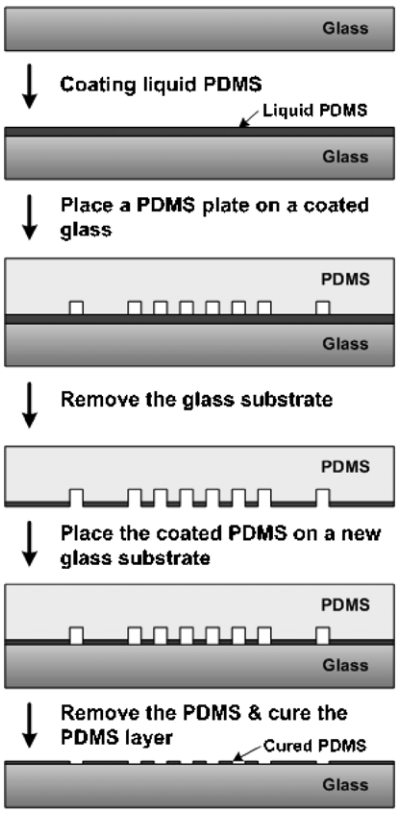

Figure 3. Fabrication procedure of patterning hydrophobic tracks and patterns on a hydrophilic surface.

3. Experimental details

3.1. Fabrication of a microfluidic device

The microfluidic patterns were fabricated with SU-8 50 photoresist (Microchem Corp) on the silicon wafers by using UV photolithography. A well-mixed liquid PDMS prepolymer (Dow Corning, Sylgard 184 A:B = 10:1) was poured onto the SU-8 master, degassed and cured in an oven at 70 °C for 1 h. The cured PDMS stamps were peeled off from the master.

Figure 3 shows the schematic illustration of patterning hydrophobic tracks and patterns by contact printing with the PDMS stamp. Hydrophobic materials for hydrophobic patterns were prepared by mixing the PDMS prepolymer and chloroform (Daejung Chemicals & Metals Co. Ltd.). Liquid PDMS diluted with chloroform was spin coated on a glass slide (Corning) at 4500 rpm for 30 s. To transfer the liquid PDMS to the PDMS stamp, the previously fabricated PDMS stamp was put on the glass slide with conformal contact for 30 s. After that, to form hydrophobic patterns and microfluidic channels on a substrate, the PDMS stamp was peeled off and put on a standard format microscope glass slide (Corning). After 30 s, the PDMS stamp was removed from the glass slide and the PDMS patterns on the glass slide were cured in an oven at 70 °C for 15 min.

Patches of adhesive tape (467 MP—50 μm thickness, 468 MP—130 μm thickness, 3 M) were attached on the glass slide as spacers. The patches were positioned at four points on the substrate to maintain the top and bottom surfaces at a fixed distance. A PMMA plate (LGMMA) with a hole was placed on the spacers as a top surface.

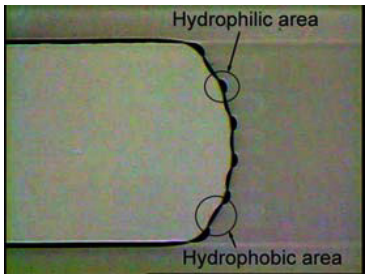

Figure 4. Optical image of liquid meniscus when liquid met the hydrophobic patterns.

3.2. Characterizaiton of a microfluidic device

To investigate the wetting property of hydrophobic patterns, contact angles of water on hydrophobic surface were measured using KRUSS G2 instrument (KRUSS). Five points were chosen for measurements and the arithmetic mean of the five values was calculated.

A stereomicroscope (SZX12, OLYMPUS) with a CCD color camera (TOSHIBA) was used to observe the movement of the liquid–gas interface. Continuous video recordings were used to analyze the position of the liquid meniscus. 10 μL distilled water was dispensed at the inlet of the microfluidc device at every measurement.

The video recordings were analyzed using an image processing software, Pinnacle Studio 8.0. The position of the liquid meniscus was determined by splitting each recording into frames. The sampling rate of video recording equipment was 30 frames sec^{-1}, corresponding to a resolution of 0.033 s.

4. Results and discussion

4.1. Hydrophobic patterning

The PDMS prepolymer was chosen for the hydrophobic material to manipulate the capillary flow because it wets most materials and has good hydrophobicity. It is difficult to directly coat the PDMS prepolymer on a glass substrate thinly because it has a high viscosity. Therefore, it was diluted with chloroform to control the thickness of hydrophobic patterns.

The thickness and dimension of PDMS patterns transferred on a glass slide varied according to the dilution factor, which is the mass ratio of chloroform to the PDMS prepolymer. To choose the appropriate dilution factor for patterning PDMS, the distance between rectangular patterns transferred on glass slides were observed by scanning electron microscopy. The results showed that the distance converged on the constant value as the dilution factor increased. From this experiment, the dilution factor of 25 was chosen because it was the beginning of the saturated value and enabled uniform transferring of liquid PDMS.

Contact angles of water to patterned PDMS, glass and PMMA were measured. Their average values were 102.3°, 24.3° and 72.0°, respectively.

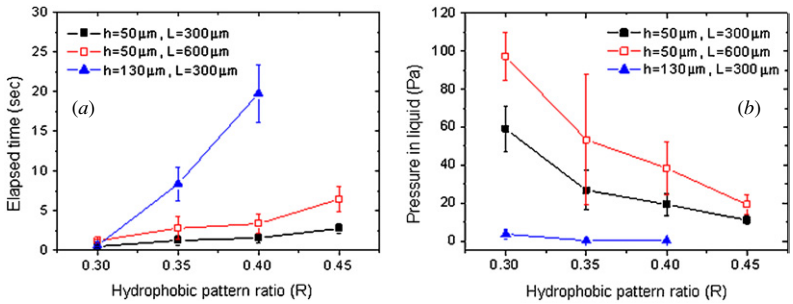

Figure 5. (*a*) Elapsed time to pass hydrophobic patterns and (*b*) pressure in liquid according to designed hydrophobic pattern ratios.

4.2. Delay of capillary flow by hydrophobic patterns

The capillary flow in a microfluidic system that was composed of hydrophobic tracks and patterns was observed using a stereomicroscopy. The hydrophilicity of top and bottom surfaces plays a vital role in the autonomous capillary flow. When glass was used for the top and bottom surfaces, the capillary flow could not be confined and spread out along the top surface which had no hydrophobic tracks. To solve this problem, PMMA substrates which have lower hydrophilicity than glass were used for the top surface.

Figure 4 shows the magnified image of liquid–gas interface when the flow was retarded by hydrophobic patterns. The interface went forward by hydrophilic surfaces whereas the interface on hydrophobic patterns formed concave lines. This phenomenon means that the local liquid pressure on hydrophilic patterns was positive whereas it was negative on hydrophobic patterns.

To show the quantitative control of the capillary flow speed, the delaying time at hydrophobic patterns was measured according to the designed hydrophobic pattern ratio, R. We also observed the effect of length of hydrophobic patterns and the gap distance between the top and bottom surfaces. Figure 5(*a*) shows the elapsed time while passing the hydrophobic patterns according to these parameters. The microchannel width, w_0, was fixed to 1 mm. As described earlier, the delaying time increased as the hydrophobic pattern ratio, the length of hydrophobic patterns and the gap distance between top and bottom surfaces increased. When R, L, and h were 0.45, 300 μm, and 50 μm, respectively, the delaying time of 3.2 s was obtained. When L was changed to 600 μm, the delaying time increased to 7.77 s. When R has changed from 0.3 to 0.45 with L being 600 μm, the delaying time has changed from 0.53 s to 3.2 s. When R, L and h was 0.5, 600 μm and 50 μm, respectively, the flow stopped in hydrophobic patterns, which resulted from the negative pressure in liquid due to increased hydrophobicitiy of surfaces. Also, when h was increased from 50 μm to 130 μm, the delaying time was increased and the flow was stopped in the case of the hydrophobic pattern ratio of 0.45.

When 10 μL distilled water was dispensed at an inlet hole, the inlet static pressure level was about 2 mm H_2O considering the geometry of the inlet hole and the volume of the dispensed drop. However, the pressure level was considered to have some fluctuations caused by the variation of the inlet hole shape, dynamics of dispensing and drop volume among the different testing cases. It is thought that the fluctuation of the inlet pressure had influence on the variation of elapsed time as shown in figure 5(*a*).

To draw the pressure in liquid from the measured delaying time at hydrophobic patterns, the Hagen–Poiseuille equation was used as the following:

$$Q = \frac{\pi R_H^4 P}{8\eta L_0}, \tag{7}$$

where Q is the volume flow rate, R_H is the hydraulic radius, L_0 is the channel length, η is the liquid viscosity and P is the pressure difference. For noncircular channels, the hydraulic radius is defined as the ratio of the cross-sectional area to the wetted perimeter. Using equation (7) and elapsed time to pass hydrophobic patterns, the pressure in liquid at hydrophobic patterns was calculated as shown in figure 5(*b*). As described earlier from equations (4) and (6), experimental data show that the pressure in liquid was close to zero, while the pressure in front of hydrophobic patterns was more than a few kPa.

However, there is some discrepancy between the simple theoretical model and experimental data. The theoretical pressure in liquid at $h = 50$ μm, $L = 300$ μm and $R = 0.3$ is 1.14 kPa from equation (6), while the experimental pressure as shown in figure 5(*b*) is 59.0 Pa. It is thought that this was because the modeling of the microfluidic system neglected the complex shape of liquid–gas interface and other forces such as friction and gravity. Furthermore, the real value of the hydrophobic pattern ratio in the experiment would be higher than the designed value as discussed earlier. Despite the difference between the theoretical model and the experimental results, this control method showed the potential to control the speed of the autonomous capillary flow by a quantitative manner. In addition, it is possible to obtain a longer delaying time according to the number of hydrophobic patterns by positioning hydrophobic patterns repeatedly along the microchannels.

Another limitation of this work is the fact that experiments were entirely done on distilled water. To verify the potential of this concept to actual applications such as biological and chemical reactions, it is necessary to test diverse solvents including physiological fluids. This is attributed to the fact that most physiological fluids have higher viscosity than water due to various biological contents. In this respect, this technique will be modified and applied to the actual microfluidic systems with physiological buffers or other viscous solutions such as serum in future works.

5. Conclusion

We have presented a theoretical and experimental method to control the speed of the autonomous capillary flow using hydrophobic patterns. A simple microfluidic device was fabricated with hydrophobic tracks and two parallel plates that were separated by a fixed distance with spacers. Hydrophobic tracks and hydrophobic patterns were made by transferring liquid PDMS onto a glass slide that was diluted with chloroform. By controlling the ratio of hydrophobic patterns to the whole channel width, R, we could control the speed of capillary flow quantitatively. The effect of the length of hydrophobic patterns and gap distance between the top and bottom surfaces was observed.

This flow control method is expected to be applicable to microfluidic systems such as micro total analysis systems or lab-on-a-chips that require a sufficient reaction time or incubation time. This method may help to increase reaction efficiency and improve the assay sensitivity.

References

[1] Sanders G H W and Manz A 2000 Chip-based microsystems for genomic and proteomic analysis *TRAC Trends Anal. Chem.* **19** 364–78

[2] Verpoorte E 2002 Microfluidic chips for clinical and forensic analysis *Electrophoresis* **23** 677–712

[3] Rossier J, Reymond F and Michel P 2002 Polymer microfluidic chips for electrochemical and biochemical analyses *Electrophoresis* **23** 858–67

[4] Juncker D, Schmid H, Drechsler U, Wolf H, Wolf M, Michel B, Rooji N and Delamarche E 2002 Autonomous microfluidic capillary system *Anal. Chem.* **74** 6139–44

[5] Unger M A, Chou H P, Thorsen T, Scherer A and Quake S R 2000 Monolithic microfabricated valves and pumps by multilayer soft lithography *Science* **288** 113–6

[6] Fahrenberg J, Bier W, Maas D, Menz W, Ruprecht R and Schomburg W K 1995 A microvalve system fabricated by thermoplastic molding *J. Micromech. Microeng.* **5** 169–71

[7] Harrison D J, Fluri K, Seiler K, Fan Z H, Effenhauser C S and Manz A 1993 Micromachining a miniaturized capillary electrophoresis-based chemical analysis system on a chip *Science* **261** 895–7

[8] Prins M W J, Welters W J J and Weekamp J W 2001 Fluid control in multichannel structures by electrocapillary pressure *Science* **291** 277–80

[9] Grant K M, Hemmert J W and White H S 2002 Magnetic field-controlled microfluidic transport *J. Am. Chem. Soc.* **124** 462–7

[10] Zhao B, Moore J S and Beebe D J 2001 Surface-directed liquid flow inside microchannels *Science* **291** 1023–6

[11] Lam P, Wynne K J and Wnek G E 2002 Surface-tension-confined microfluidics *Langmuir* **18** 948–51

[12] Bouaidat S, Hansen O, Bruus H, Berendsen C, Bau-Madsen N K, Thomsen P, Wolff A and Jonsmann J 2005 Surface-directed capillary system: theory, experiments and applications *Lab. Chip.* **5** 827–36

[13] Man P F, Mastrangelo C H, Burns M A and Burke D T 1998 Microfabricated capillary-driven stop valve and sample injector *MEMS '98* pp 45–50

[14] Leu T and Chang P 2004 Pressure barrier of capillary stop valves in micro sample separators *Sensors Actuators* A **115** 508–15

[15] Handique K, Burke D T, Mastrangelo C H and Burns M A 2000 Nanoliter liquid metering in microchannels using hydrophobic patterns *Anal. Chem.* **72** 4100–9

[16] Andersson H, Wijngaart W, Griss P, Niklaus F and Stemme G 2001 Hydrophobic valves of plasma deposited octafluorocyclobutane in DRIE channels *Sensors Actuators* B **75** 136–41

[17] Rossier J S, Gokulrangan G, Girault H H, Svojanovsky S and Wilson G S 2000 Characterization of protein adsorption and immunosorption kinetics in photoablated polymer microchannels *Langmuir* **16** 8489–94

[18] Lai S, Wang S, Luo J, Lee L J, Yang S and Madou M J 2004 Design of a compact disk-like microfluidic platform for enzyme-linked immunosorbent assay *Anal. Chem.* **76** 1832–7